

# Mo<sub>1-x</sub>W<sub>x</sub>S<sub>2</sub> nanotubes and related structures

Manashi Nath<sup>a,b</sup>, K. Mukhopadhyay<sup>a</sup>, C.N.R. Rao<sup>a,b,\*</sup>

<sup>a</sup> *Chemistry and Physics of Materials Unit, CSIR Center of Excellence in Chemistry, Jawaharlal Nehru Centre for Advanced Scientific Research, Jakkur P.O., Bangalore 560 064, India*

<sup>b</sup> *Solid State and Structural Chemistry Unit, Indian Institute of Science, Bangalore 560 012, India*

Received 2 October 2001; in final form 4 December 2001

## Abstract

(NH<sub>4</sub>)<sub>2</sub>MoS<sub>4</sub> and (NH<sub>4</sub>)<sub>2</sub>WS<sub>4</sub> form solid solutions over the entire composition range. Nanotubes of Mo<sub>1-x</sub>W<sub>x</sub>S<sub>2</sub> solid solutions have been prepared by employing these solid solutions precursors. Thus, the thermal decomposition of (NH<sub>4</sub>)<sub>2</sub>Mo<sub>1-x</sub>W<sub>x</sub>S<sub>4</sub> in an inert or a hydrogen atmosphere yields Mo<sub>1-x</sub>W<sub>x</sub>S<sub>2</sub> nanotubes, those with  $x < 0.1$  being more readily obtained. The nanotubes exhibit novel tip architectures and defects. Single-walled nanotubes have also been observed in some samples. © 2002 Published by Elsevier Science B.V.

## 1. Introduction

Since Tenne et al. [1] established that layered sulfides such as MoS<sub>2</sub> and WS<sub>2</sub> form nanotubes and other fullerene type structures, there has been considerable effort to synthesize and characterize nanotubes of a variety of inorganic layered materials [2,3]. Besides developing strategies for synthesizing such novel nanotubes, there have been attempts to substitute Mo and W in MoS<sub>2</sub> and WS<sub>2</sub> nanotubes by other metals. Thus, Ti has been introduced in MoS<sub>2</sub> nanotubes, starting with a Mo–Ti alloy [4]. Nb-doped WS<sub>2</sub> nanotubes have been prepared starting with Nb<sub>2</sub>O<sub>5</sub> covered WO<sub>x</sub> [5]. Mixed phase W<sub>x</sub>Mo<sub>y</sub>C<sub>z</sub>S<sub>2</sub> nanotubes [6] have been prepared by passing H<sub>2</sub>S over a mixture of carbon with Mo and W oxides around 950 °C. In

spite of these useful contributions, nanotubes of solid solutions of MoS<sub>2</sub> and WS<sub>2</sub> have not been prepared and characterized hitherto. Such Mo<sub>1-x</sub>W<sub>x</sub>S<sub>2</sub> nanotubes would be expected to have different tribological and other properties compared to MoS<sub>2</sub> and WS<sub>2</sub>. In order to prepare Mo<sub>1-x</sub>W<sub>x</sub>S<sub>2</sub> nanotubes, we have employed the pyrolysis of ammonium thiometallates [7], since (NH<sub>4</sub>)<sub>2</sub>MoS<sub>4</sub> and (NH<sub>4</sub>)<sub>2</sub>WS<sub>4</sub> form solid solutions over the entire composition range. By carrying out the pyrolysis of the ammonium thiometallate solid solutions in an inert atmosphere, we have been able to prepare Mo<sub>1-x</sub>W<sub>x</sub>S<sub>2</sub> nanotubes of a few compositions. We report preliminary results of our findings in this Letter.

## 2. Experimental

(NH<sub>4</sub>)<sub>2</sub>MoS<sub>4</sub> and (NH<sub>4</sub>)<sub>2</sub>WS<sub>4</sub> form solid solutions, (NH<sub>4</sub>)<sub>2</sub>Mo<sub>1-x</sub>W<sub>x</sub>S<sub>4</sub>, over the entire compo-

\* Corresponding author. Fax: +91-80-8462760.

E-mail address: cnrrao@jncasr.ac.in (C.N.R. Rao).

sition range, ( $0 \leq x \leq 1$ ). The  $(\text{NH}_4)_2\text{Mo}_{1-x}\text{W}_x\text{S}_4$  compositions were prepared as follows.  $(\text{NH}_4)_2\text{MoO}_4$  was dissolved in distilled water containing few milliliters of ammonia. To this so-

lution was added a suspension of  $(\text{NH}_4)_2\text{WO}_4$  in ammoniacal water.  $\text{H}_2\text{S}$  was bubbled through the mixture (with slight warming when  $x$  was less than 0.05). A color change was observed first to yellow

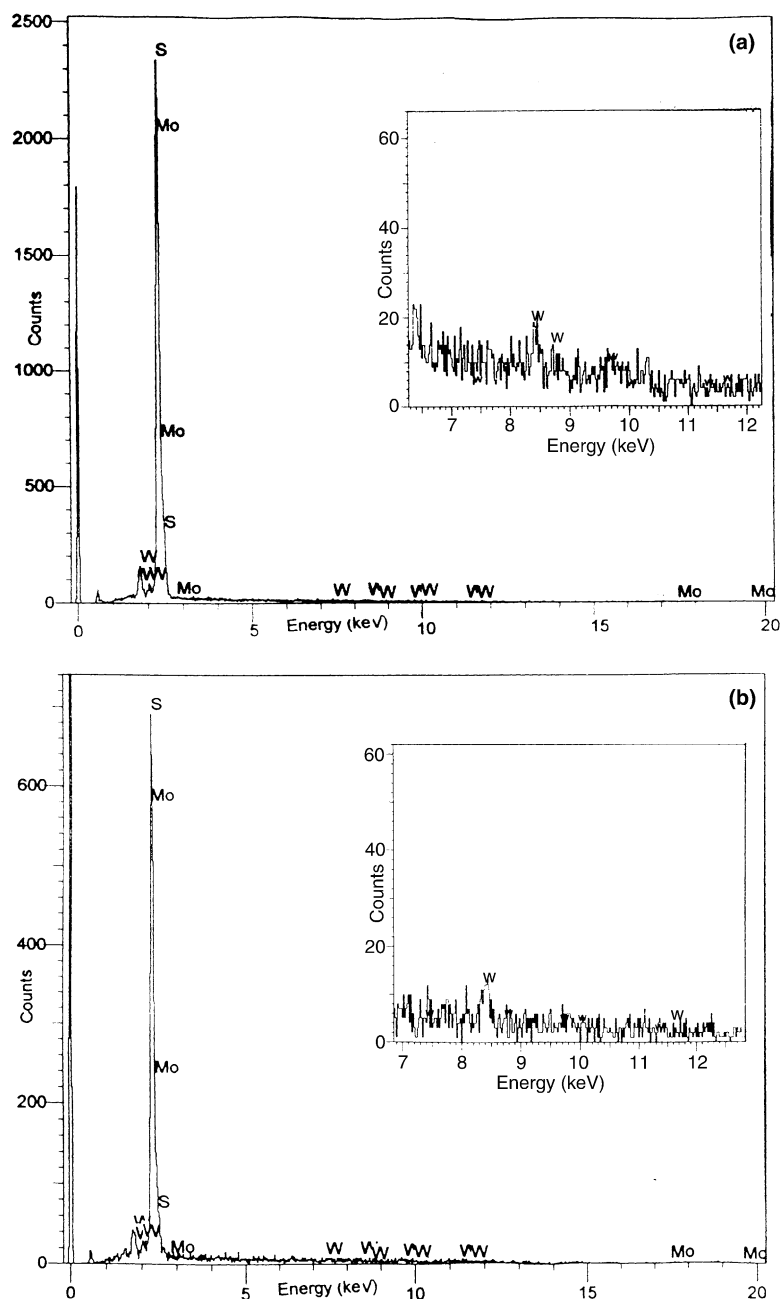
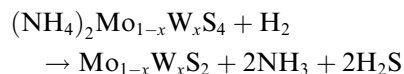
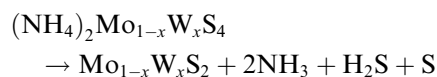


Fig. 1. EDAX patterns of (a)  $(\text{NH}_4)_2\text{Mo}_{1-x}\text{W}_x\text{S}_4$  and (b)  $\text{Mo}_{1-x}\text{W}_x\text{S}_2$  nanotubes ( $x \approx 0.06$ ).

and subsequently to red (for  $x < 0.09$ ). The precipitates were collected, filtered and washed with deionized water and dried. The final compositions of the thiometallate solid solutions were ascertained from EDAX analysis. These solid solutions were X-ray amorphous. The proportion of ammonium molybdate and ammonium tungstate taken initially influences the final composition of  $(\text{NH}_4)_2\text{Mo}_{1-x}\text{W}_x\text{S}_4$ . In order to obtain  $x > 0.09$ , an excess of  $(\text{NH}_4)_2\text{WO}_4$  had to be taken in the initial reaction mixture.

The thiometallate solid solutions were pyrolysed in a quartz tube of 17 mm diameter placed in a tubular furnace. The quartz boat containing the thiometallate precursor was kept in the central zone of the furnace and an inert gas (Ar, He or  $\text{N}_2$ ) or hydrogen was passed through it ( $\sim 150$  sccm). The temperature of the furnace was maintained at 1043 K for 1–1.5 h. Placing a small amount of sulfur powder near the inlet of the furnace, such that the sulfur vapors were carried by the gas, resulted in a noticeable increase in the yield of the nanostructures.

X-ray diffraction patterns of the products showed characteristic reflections of the layered structures. EDAX analysis gave Mo:W ratios expected on the basis of the starting compositions of the thiometallates. In Fig. 1 we show the EDAX patterns of a thiometallate solid solution and the  $\text{Mo}_{1-x}\text{W}_x\text{S}_2$  nanostructure obtained from it. The Mo:W ratio is 15:1 in the thiometallate, and 14:1 in the disulfide solid solution. Such a satisfactory stoichiometry of the nanostructures validate the method of preparation. The reactions involved in the formation of the disulfide is given by



### 3. Results and discussion

We could obtain good yields of the  $\text{Mo}_{1-x}\text{W}_x\text{S}_2$  nanotubes with  $x < 0.1$ , but the yield decreases to

some extent with increase in  $x$ , possibly because such a substitution increases the strain in the disulfide layers. EXAFS and related studies [8] have shown that W substitution occurs in the  $\text{MoS}_2$  layer and that both the cations are present in the layers of  $\text{Mo}_{1-x}\text{W}_x\text{S}_2$  solid solutions. The inter-layer separation remains at 0.62 nm in the nanotubes with  $x < 0.1$

In Figs. 2a and b, we show high resolution TEM (HREM) images of  $\text{Mo}_{1-x}\text{W}_x\text{S}_2$  ( $x = 0.06$ ) nanotubes with external diameters of 24 and 27 nm and inner core diameters of 9 and 8 nm, respectively. The closed spherical tips are similar to those commonly found in carbon nanotubes. There are layer defects at the tip and along the walls. We also observe novel tip architectures in the nanotubes as revealed in Fig. 3. The nanotube in Fig. 3a with an external diameter of  $\sim 150$  nm has a rectangular tip with sharp  $90^\circ$  bends inside (near the core), and

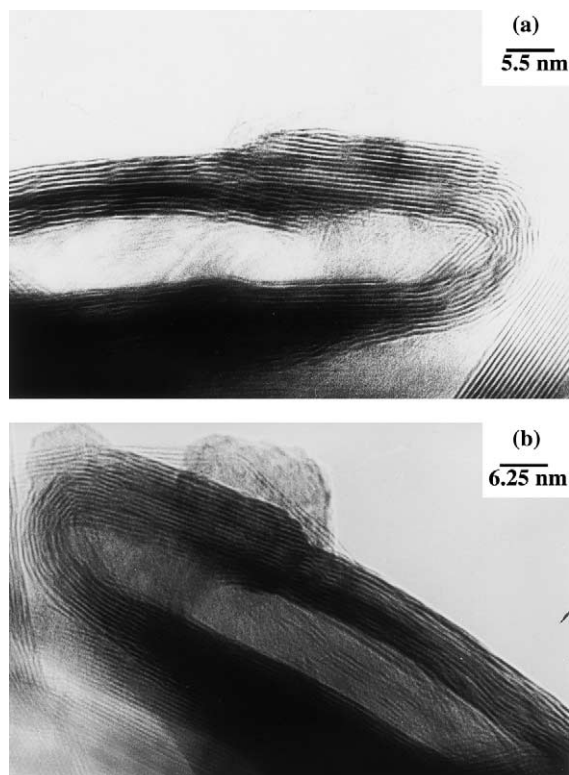


Fig. 2. (a), (b) HREM images of  $\text{Mo}_{0.94}\text{W}_{0.06}\text{S}_2$  nanotubes with spherical tips and showing a layer separation of  $\sim 0.62$  nm.

smooth corners at the outer edges. The outer layers at the tip show discontinuity in some regions and there are layer defects and dislocations causing deformation in layer stacking. The defects found by us in the  $\text{Mo}_{1-x}\text{W}_x\text{S}_2$  nanotubes are similar to those described in  $\text{WS}_2$  and  $\text{MoS}_2$  nanotubes by Walton, Kroto and coworkers [3,4,9]. The TEM image of the nanotube ( $x = 0.06$ ) in Fig. 3b is unusual in that the diameter decreases from  $\sim 55$  nm to 40 nm near the tip. The tip itself is non-spherical and polygonal with a  $\sim 90^\circ$  bend at one end. In spite of the large diameter, the tube wall comprises 10–12 layers only. The number of layers on either side of the core is different, unlike in carbon nanotubes. There are layer defects along the walls and the growth of some of the layers terminates near the tip.

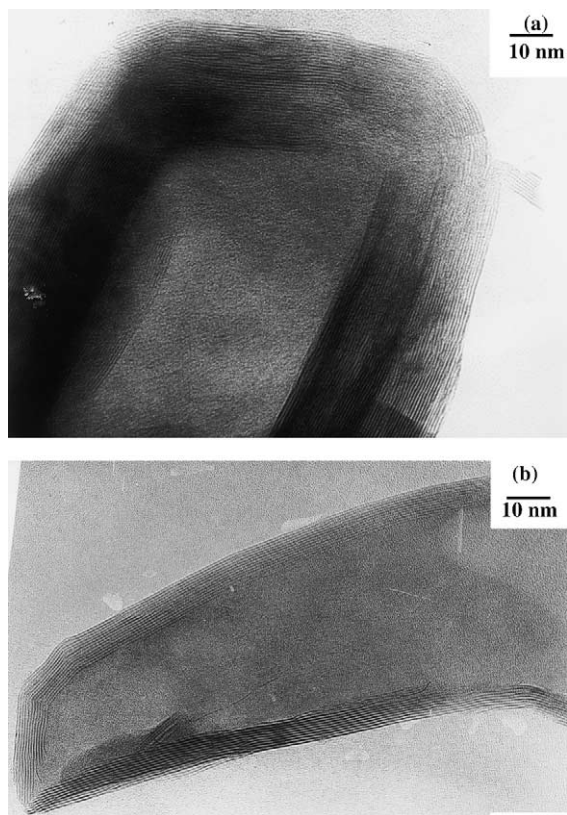


Fig. 3. HREM images of  $\text{Mo}_{0.94}\text{W}_{0.06}\text{S}_2$  nanotubes showing (a) near-rectangular tip and (b) a polygonal tip with  $\sim 90^\circ$  bend at one corner.

In Fig. 4a we show a TEM image of what appears to be a bundle of single-walled nanotubes with  $x = 0.05$ , not unlike that of  $\text{MoS}_2$  reported by Remskar et al. [10]. The image of the nanotube in Fig. 4b reveals a near-conical tip with a bamboo type structure reported earlier in carbon and BN nanotubes [11,12]. Such polygonal or conical tips could arise from rhombohedral or triangular point defects in the disulfide nanotubes. Here again, we

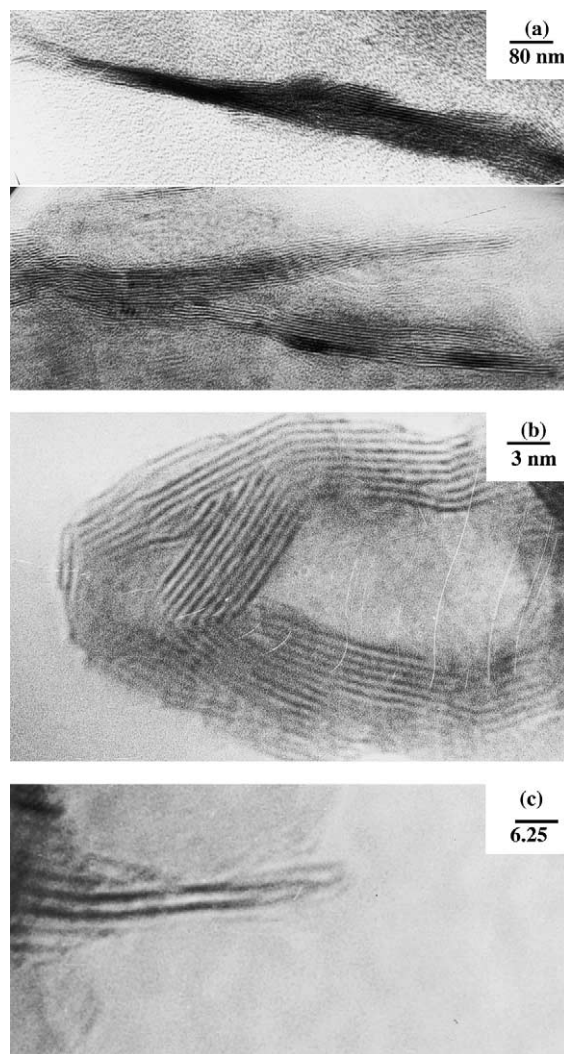


Fig. 4. HREM images of  $\text{Mo}_{1-x}\text{W}_x\text{S}_2$  ( $x = 0.05$ ) nanotubes: (a) bundles of single-walled nanotubes; (b) a nanotube with a bamboo-like morphology; (c) a single-walled nanotube structure. The layer separation in (b) is  $\sim 0.62$  nm.

see the number of layers near the tip to be different from that along the walls, suggesting that a simultaneous growth mechanism may be operative

[9]. We have found occasional single-walled nanotube structures of the type shown in Fig. 4c, with a separation of 1.4 nm.

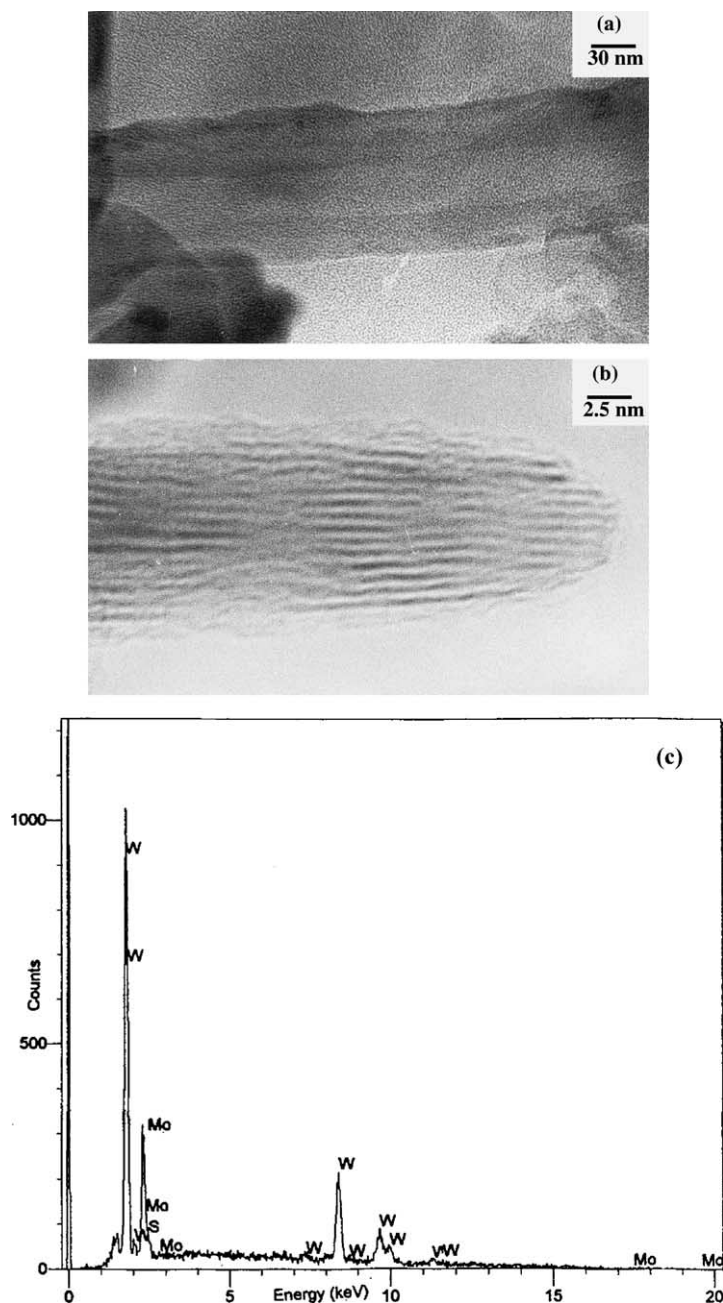


Fig. 5. (a) Low resolution TEM image of a  $\text{Mo}_{0.5}\text{W}_{0.5}\text{S}_2$  nanotube; (b) TEM image of a  $\text{Mo}_{0.5}\text{W}_{0.5}\text{S}_2$  nanorod with a layer separation of  $\sim 0.62$  nm; (c) the EDAX pattern of the  $\text{Mo}_{0.5}\text{W}_{0.5}\text{S}_2$  nanostructure.

The electron diffraction patterns obtained from the nanotubes in the present study shows them to be mostly of the armchair and zigzag type [13]. The tube closure occurs by the presence of defects in the growing chalcogenide layers viz. the triangular or rhombohedral point defects in the  $\text{MX}_2$  dichalcogenide layer leading to curvature [14]. Topological defect like three or four square-like defects and one octagonal-like defect can close the armchair and zigzag tubes, respectively [13]. In the present study, it has been observed that some of the tubes have a rectangular tip (see Fig. 3a), indicating the presence of a rhombohedral point defect as has been suggested by Tenne [14] for a rectangular inorganic fullerene. It seems possible that the intra-layer doping of W in the predominantly  $\text{MoS}_2$  may lead to increased strain in the order and orientation of stacking leading to termination of growth of some of the layers. An increased proportion of W in the  $\text{MoS}_2$  layers would lead to more of point defects, thereby forming more faceted tips with sharp bends at the edges.

The yield of the  $\text{Mo}_{1-x}\text{W}_x\text{S}_2$  nanotubes varies with  $x$  and decreases with the increasing content of tungsten. Besides the nanotubes, other nanostructures like nanorods, nanowires and inorganic fullerenes are also obtained. The highest yield of these nanostructures (obtained for  $\text{Mo}_{0.95}\text{W}_{0.05}\text{S}_2$ ) was  $\sim 60$ – $70\%$ . Out of these nearly  $20\%$  was nanotubes.

In conclusion, we have been able to prepare  $\text{Mo}_{1-x}\text{W}_x\text{S}_2$  nanotubes by the decomposition of thiometallate solid solutions of the formula  $(\text{NH}_4)_2\text{Mo}_{1-x}\text{W}_x\text{S}_4$ . A high proportion of the nanotubes with  $x < 0.1$  had closed tips with a variety of architectures. Although we have only described the nanotubes with small  $x$  in some detail, we have obtained a few nanotubes in the composition range  $0.1 \leq x \leq 0.6$  in low yields. We show a low resolution TEM image of a nanotube with  $x = 0.6$  in Fig. 5 along with the EDAX pattern. The figure also shows the image of a nanorod of this solid solution. The nanotube has an outer diameter of

93 nm and an inner core diameter of 33 nm. Further studies on the  $\text{Mo}_{1-x}\text{W}_x\text{S}_2$  nanotubes are in progress.

### Acknowledgements

The authors thank DRDO (India) for support.

### References

- [1] R. Tenne, L. Margulis, M. Genut, G. Hodes, *Nature* 360 (1992) 444.
- [2] C.N.R. Rao, B.C. Satishkumar, A. Govindaraj, M. Nath, *Chem. Phys. Chem.* 2 (2001) 78.
- [3] R. Tenne, in: K.D. Kerlin (Ed.), *Progress in Inorganic Chemistry*, 50, John Wiley & Sons, New York, 2001, p. 269.
- [4] W.K. Hsu, Y.Q. Zhu, N. Yao, S. Firth, R.J.H. Clark, H.W. Kroto, D.R.M. Walton, *Adv. Funct. Mater.* 11 (2001) 69.
- [5] W.K. Hsu, Y.Q. Zhu, S. Firth, M. Terrones, R.J.H. Clark, H.W. Kroto, D.R.M. Walton, *Chem. Phys. Lett.* 342 (2001) 15.
- [6] W.K. Hsu, Y.Q. Zhu, C.B. Boothroyd, I. Kinloch, S. Trasobares, H. Terrones, N. Grobert, M. Terrones, R. Escudero, G.Z. Chen, C. Colliex, A.H. Windle, D.J. Fray, H.W. Kroto, D.R.M. Walton, *Chem. Mater.* 12 (2000) 3541.
- [7] M. Nath, A. Govindaraj, C.N.R. Rao, *Adv. Mater.* 13 (2001) 283.
- [8] C. Thomazeau, C. Geantet, M. Lacroix, V. Harle, S. Benazeth, C. Marhic, M. Danot, *J. Solid State Chem.* 160 (2001) 147.
- [9] Y.Q. Zhu, W.K. Hsu, H. Terrones, N. Grobert, B. Chang, M. Terrones, B.Q. Wei, H.W. Kroto, D.R.M. Walton, C.B. Boothroyd, I. Kinloch, G.Z. Chen, A.H. Windle, D.J. Fray, *J. Mater. Chem.* 10 (2000) 2570.
- [10] M. Remskar, A. Mrzel, Z. Skraba, A. Jesih, M. Ceh, J. Demšar, P. Stadelman, F. Levy, D. Mihailovic, *Science* 292 (2001) 479.
- [11] C.J. Lee, J.H. Park, J. Park, *Chem. Phys. Lett.* 323 (2000) 560.
- [12] X. Ma, E.G. Wang, *Appl Phys. Lett.* 78 (2001) 978.
- [13] G. Seifert, H. Terrones, M. Terrones, G. Jungnickel, T. Frauenheim, *Phys. Rev. Lett.* 85 (2000) 146.
- [14] R. Tenne, M. Homyonfer, Y. Feldman, *Chem. Mater.* 10 (1998) 3225.